# Neutron star long term cooling -
# Joule heating in magnetized neutron stars

**Deborah N. Aguilera**[*][†]
*Departamento de Física Aplicada. Universidad de Alicante, Spain*
*E-mail:* deborah.aguilera@ua.es

**José A. Pons**
*Departamento de Física Aplicada. Universidad de Alicante, Spain*
*E-mail:* jose.pons@ua.es

**Juan A. Miralles**
*Departamento de Física Aplicada. Universidad de Alicante, Spain*
*E-mail:* ja.miralles@ua.es

We present two-dimensional simulations for the cooling of neutron stars with strong magnetic fields ($B \geq 10^{13}$ G). We study how the cooling curves are influenced by magnetic field decay. We show that the Joule heating effects are very large and in some cases control the thermal evolution. We characterize the temperature anisotropy induced by the magnetic field and predict the surface temperature distribution for early and late stages of the evolution of isolated neutron stars, comparing our results with available observational data of isolated neutron stars.

*Supernovae: lights in the darkness*
*October 3-5, 2007*
*Maó (Menorca)*

[*]Speaker.

[†]Present address: Theoretical Physics, Tandar Laboratory, Comisión Nacional de Energía Atómica (CNEA-CONICET), Av. Gral. Paz 1499, 1650 San Martín, Pcia. Buenos Aires, Argentina

## 1. Introduction

Recently, observational data of thermally emitting isolated neutron stars (NSs) confirm that most of them have magnetic fields larger than $10^{13}$ G. Therefore, a reliable treatment of the thermal evolution must not avoid the inclusion of the effects produced by the presence of high magnetic fields.

The non-uniform distribution of the surface temperature of isolated NSs seems to be confirmed by the analysis of observational data (see reviews [1] and [2]). The mismatch between the extrapolation to low energy of the fits to X-ray spectra, and the observed Rayleigh Jeans tail in the optical band (*optical excess flux*), cannot be addressed with a uniform temperature. Several simultaneous fits to multiwavelength spectra of RX J1856.5−3754 [3], RBS 1223 [4], and RX J0720.4−3125 [5] are explained by a small hot emitting area $\simeq$ 10–20 km$^2$ and an extended cooler component.

The non-uniform surface temperature distribution may be produced by crustal confined magnetic fields [6, 7]. Magnetic fields larger than $10^{13}$ G limit the movement of the electrons (heat carriers) in the direction perpendicular to the field with the result that the thermal conductivity is highly suppressed, while remains almost unaffected along the field lines.

For such large fields, the field decay through Ohmic dissipation and Hall drift processes is very efficient and the heat released in the crust (Joule heating) must be taken into account in the thermal evolution of a neutron star [8]. In this article we focused on the effects of field decay and Joule heating on the neutron star cooling. In particular, we compare our simulations with observational data of a sample of isolated NSs that are highly magnetized.

## 2. Cooling of neutron stars with magnetic fields

We have performed two–dimensional simulations by solving the energy balance equation that describes the thermal evolution of a neutron star (NS)

$$C_v \frac{\partial T}{\partial t} - \vec{\nabla} \cdot (\hat{\kappa} \cdot \vec{\nabla} T) = -Q_v + Q_J \, , \tag{2.1}$$

where $C_v$ is the specific heat per unit volume, $Q_v$ are energy losses by $v$-emission, $Q_J$ the heat released by Joule effect, and $\hat{\kappa}$ is the thermal conductivity tensor, in general anisotropic in presence of a magnetic field. In this equation we have omitted relativistic factors for simplicity. A detailed description of the formalism, the code, and results can be found in [8]. The geometry of the magnetic field is fixed during the evolution. As a phenomenological description of the field decay, we have assumed the following law

$$B = B_0 \frac{\exp(-t/\tau_{\text{Ohm}})}{1 + (\tau_{\text{Ohm}}/\tau_{\text{Hall}})(1 - \exp(-t/\tau_{\text{Ohm}}))} \, , \tag{2.2}$$

where $B$ is the magnetic field at the pole, $B_0$ its initial value, $\tau_{\text{Ohm}}$ is the Ohmic characteristic time, and $\tau_{\text{Hall}}$ the typical timescale of the fast, initial Hall stage. In the early evolution, when $t \ll \tau_{\text{Ohm}}$, we have $B \simeq B_0(1 + t/\tau_{\text{Hall}})^{-1}$ while for late stages, when $t \geq \tau_{\text{Ohm}}$, $B \simeq B_0 \exp(-t/\tau_{\text{Ohm}})$. This simple law reproduces qualitatively the results from more complex simulations [9] and facilitates the implementation of field decay in the cooling of NSs for different Ohmic and Hall timescales.

## 3. Joule heating governing the cooling

Given a 1.35 $M_\odot$ neutron star model with a crustal confined magnetic field as in [8], we have varied the parameters that describe the typical timescales for Ohmic dissipation and a fast initial decay induced by the Hall drift.
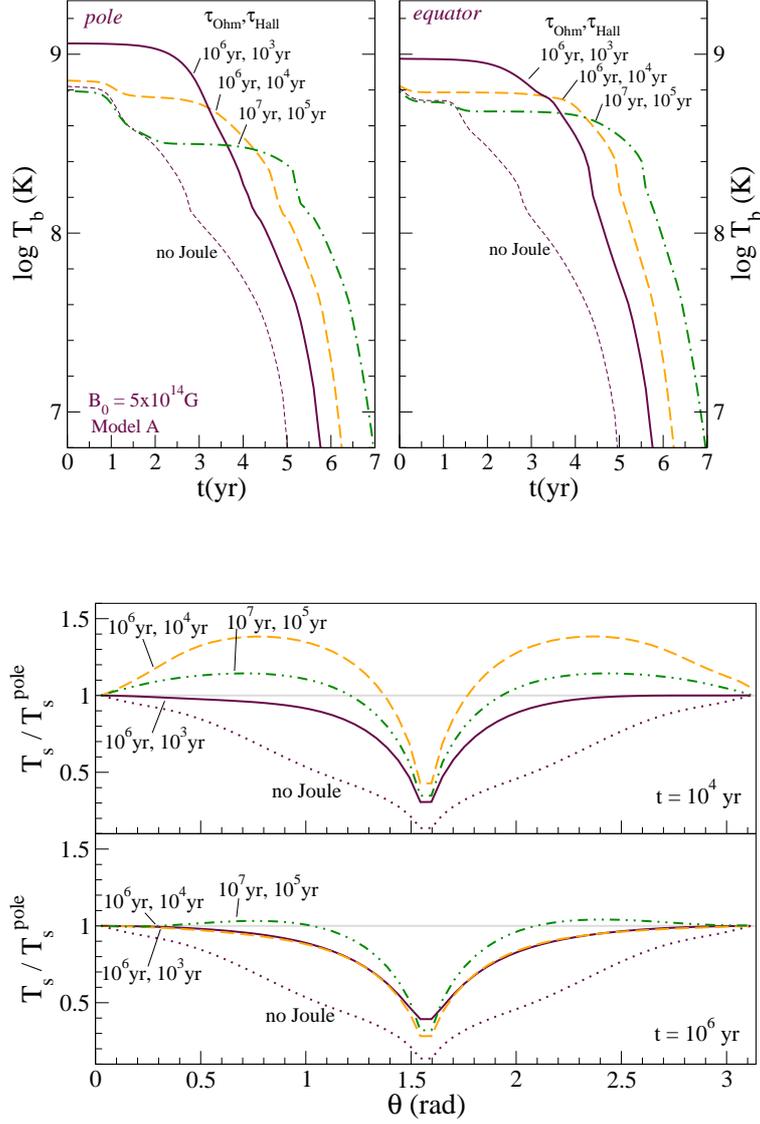


**Figure 1:** Cooling of strongly magnetized NSs with Joule heating for $B_0 = 5 \times 10^{14}$ G. Upper panel shows $T_b$ vs. $t$ at the pole (left) and at the equator (right). Lower panel shows $T_s$ normalized to its value at the pole vs. $\theta$. Three pairs of Joule parameters $\tau_{Ohm}, \tau_{Hall}$ are shown: $10^6$yr, $10^3$yr (solid lines), $10^6$yr, $10^4$yr (dashed lines), and $10^7$yr, $10^5$yr (dotted dashed lines), respectively

In Fig. 1 (upper panel) we show the cooling curves, the temperature at the bottom of the envelope, $T_b$, as a function of the age $t$ for three different pairs of values ($\tau_{Ohm}, \tau_{Hall}$): ($10^6$yr, $10^3$yr),

($10^6$yr, $10^4$yr), and ($10^7$yr, $10^5$yr) represented by solid lines, dashed lines, and dash-dotted lines, respectively. For comparison, the thin dashed lines show the evolution with constant field for the same initial field $B_0 = 5 \times 10^{14}$ G.

It is first to notice that there is a large effect on $T_b$: as a consequence of the heat released, it remains much higher than in the case of non–decaying magnetic field. The strong influence of the field decay is evident for all parameters chosen. The temperature of the initial plateau is higher for shorter $\tau_{\text{Hall}}$, but the duration of this stage with nearly constant temperature is also shorter. When $t = \tau_{\text{Hall}}$, $B$ has decayed to about $1/2 B_0$ and $3/4$ of the initial magnetic energy has been dissipated, so that reducing $\tau_{\text{Hall}}$ we can keep higher temperatures, but for shorter times. After $t = \tau_{\text{Hall}}$, $T_b$ drops due to the transition from the fast Hall decay to the slower Ohmic decay.

The insulating effect of tangential magnetic fields is twofold. First, in the absence of additional heating sources, it decouples low latitude regions from the hotter core resulting in lower temperatures at the base of the envelope. Second; if there is heat released in the crust, it prevents the extra heat to flow into the inner crust or the core where it is more easily lost in the form of neutrinos. Our simulations with Joule heating show systematically a hot equatorial belt at the crust–envelope interface. However, as discussed in [8], the *inverted temperature distribution* at the level of the crust is not necessarily visible in the surface temperature, $T_s$, distribution because it is filtered by the magnetized envelope. An analysis of the angular temperature distribution given in the lower panel of Fig. 1 shows the development of a middle latitude region hotter than the pole at relatively late stages in the evolution ($t \simeq 10^4 - 10^5$ yr). This hotter area is found with a wide range of parameters, and it would have implications on the light curves of rotating NSs, that will differ substantially from the light curves obtained with a typical hot polar cap model.

## 4. Comments on the spin-down age of NSs

Another aspect that should be reconsidered when we try to fit cooling curves to explain observations is that for many objects the age is calculated from the measurements of the rotational period $P$ and its derivative $\dot{P}$. The *spin down age*, $t_{sd} = P/2\dot{P}$, is derived assuming that the lose of angular momentum is entirely due to dipolar radiation from a constant (in time) magnetic dipole. In the case of a decaying magnetic field, $t_{sd}$ can seriously overestimate the *true age $t$*. A simple algebra shows that in the case of purely Ohmic decay

$$t = \frac{\tau_{\text{Ohm}}}{2} \ln\left(1 + 2\frac{t_{\text{sd}}}{\tau_{\text{Ohm}}}\right). \tag{4.1}$$

In the case that a Hall–induced fast decay also occurs, Eq. (2.2) results in a large correction of $t_{\text{sd}}$ as follows:

$$t_{\text{sd}} = \tau_{\text{Hall}}\, f(t)\, e^{2t/\tau_{\text{Ohm}}} \left[ f(t) - e^{-t/\tau_{\text{Ohm}}} - \frac{\tau_{\text{Hall}}}{\tau_{\text{Ohm}}} f(t) \ln f(t) \right] \tag{4.2}$$

where $f(t) = 1 + \frac{\tau_{\text{Ohm}}}{\tau_{\text{Hall}}}(1 - e^{-t/\tau_{\text{Ohm}}})$. This relation gives $t_{\text{sd}} \gg t$ by several orders of magnitude for $t \gg \tau_{\text{Hall}}$, as shown in Fig. 2. Therefore, the cooling evolution time should be corrected according to the prescription for the magnetic field decay in order to compare with the observations properly. A detailed comparison with observational sources is presented in [10] and is summarized in the next section.
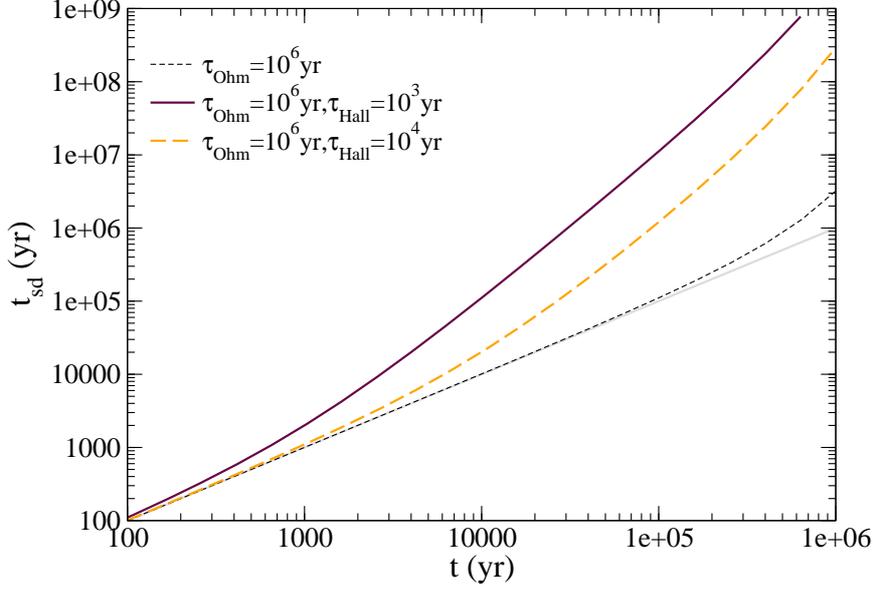
**Figure 2:** Spin down age ($t_{sd}$) vs. *true age* ($t$) for a model with magnetic field decay. Results for two rates ($\tau_{Ohm}, \tau_{Hall}$) are shown: $(10^6, 10^3)$ yr (solid lines) and $(10^6, 10^4)$ yr (dashed lines). The grey solid line represents $t_{sd} = t$, and the short dashed line the purely Ohmic decay with $\tau_{Ohm} = 10^6$ yr.

## 5. Comparison with observations

We compare in Fig. 3 our simulations with observational data of NSs covering about three orders of magnitude in magnetic field strength: from radio-pulsars ($B \simeq 10^{12}$ G) and isolated radio-quiet NSs ($B \simeq 10^{13}$ G) to recent magnetar candidates ($B \simeq 10^{14-15}$ G). The sources considered here are listed in Table 1 of [10], with the corresponding references.

For most NSs, $B$ is estimated by assuming that the lose of angular momentum is entirely due to dipolar radiation. The dipolar component is $B_d = 3.2 \times 10^{19}(P\dot{P})^{1/2}$ G, where $P$ is the spin period in seconds, and $\dot{P}$ is its time derivative. In order to work with an homogeneous sample, we have included in the comparison only those objects for which $\dot{P}$ is available and the quoted magnetic field is $B_d$ and discarded those sources for which the magnetic field is inferred by other methods[1].

The reported temperatures are in most cases blackbody temperatures, except for low field radio-pulsars for which we take the temperature consistent with Hydrogen atmospheres following the criteria in [11]. Nevertheless, there are some objects in which the estimate is an upper limit for the thermal component, like the Crab pulsar. This is also the case for some magnetars, which show large variations in the flux in the soft x-ray band on a timescale of a few years, indicating that the thermal component must be measured during quiescence and that the luminosity during their active periods is a result of magnetospheric activity.

The age of a NS is subject to a large uncertainty, but it can be estimated by the *spin-down age*,

---

[1]For a few radio-quiet isolated NSs $B$ can also be estimated assuming that observed x-ray absorption features are due to proton cyclotron lines, but this gives the surface field, which is usually larger than the external dipolar component
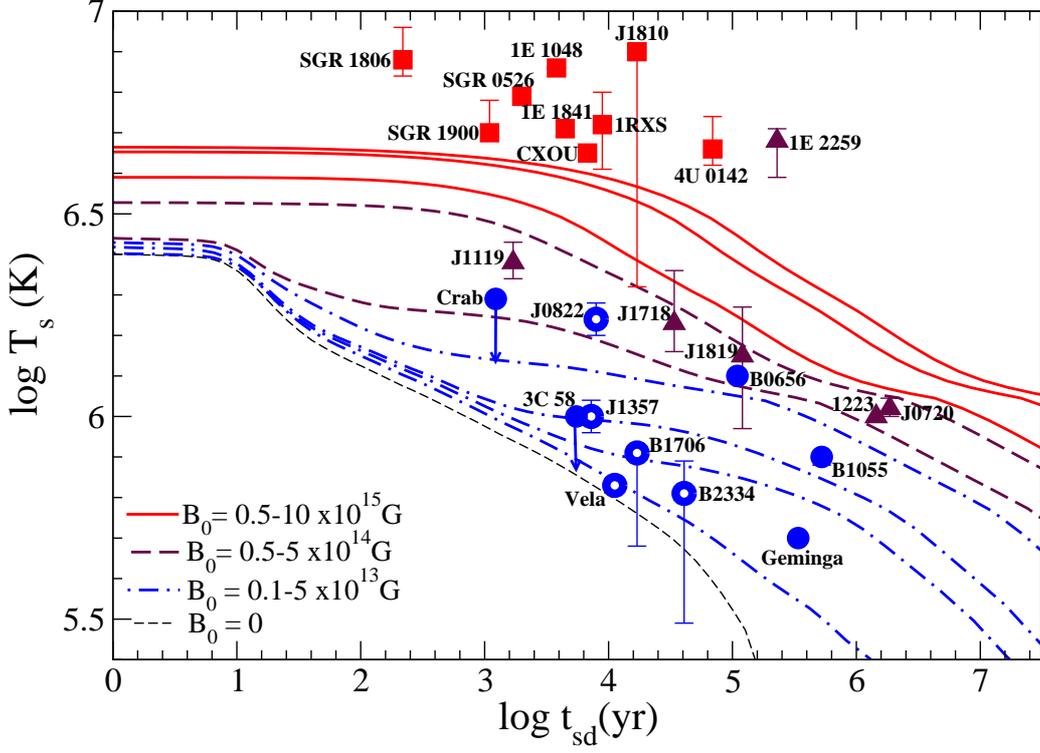
**Figure 3:** Cooling curves, $T_s$ vs. corrected spin down age $t_{sd}$. Observational sources correspond to Table 1 of [10]. Symbols identify sources with the same order of magnetic field: squares for magnetars (AXPs and SGRs, with $B \simeq 10^{14-15}$ G), triangles for radio-quiet isolated NSs (with $B \simeq 10^{13}$ G), and circles for radio-pulsars (with $B \simeq 10^{12}$ G). Open circles denote temperatures obtained from fits to Hydrogen atmospheres.

$t_{sd}$, provided that the birth spin rate far exceeds the present spin rate and $B$ is considered constant[2]. As shown in Sec. 2, if one considers magnetic field decay, $t_{sd}$ seriously overestimates the age $t$ of the simulations. Therefore, we transform the cooling curves to plot $T_s$ vs. $t_{sd}$, to include the temporal variation of the magnetic field.

In Fig. 3 our results show that the effect of high magnetic field ($B_0 \simeq 10^{14-15}$ G, solid lines) in the cooling is important from the very beginning of the NS evolution. The temperature reached is increased up to a factor of 5 in comparison with a non–magnetized model and can be kept nearly constant for about $10^4$ years. The effect of Joule heating is very significant and may help to explain why magnetars are so hot [12]: the high temperatures in the early epoch result in higher electrical resistivity and in an faster magnetic field dissipation that releases the heat in the crust. In this picture, the thermal evolution of radio-quiet, isolated NSs could be represented either by NSs born with intermediate fields in the range of $B_0 = 10^{13-14}$ G (dashed lines) or by magnetars in which the field has already decayed in a timescale of $\approx 10^{5-6}$ years. For intermediate field strengths, the initial effect is not so pronounced but the star can be kept much hotter than non-magnetized

---

[2]For some cases an independent *kinematic age* is available, which does not necessarily coincide with $t_{sd}$.

NSs from $10^4$ yr to $10^6$ yrs. For weakly magnetized NSs, radiopulsars with $B \simeq 10^{12}$ G, the effect of the magnetic field is small (dashed dotted lines) and they can satisfactorily be explained by non-magnetized models, with the exception of very old objects ($t > 10^6$ years), as discussed in [13].

## 6. Conclusions

From the results presented here we conclude that the thermal evolution of a magnetized NSs is strongly affected by the presence of magnetic fields. Therefore, studies aimed to disentangle properties of NSs interior (e.g. EoS, neutrino processes, etc.) for objects with $B \geq 10^{13}$ G, through cooling curves should not neglect the (dominant) magnetic field effects. A first step towards a coupled magneto-thermal evolution has been given in this work and future investigations will consider a consistent evolution including the evolution of the magnetic field geometry.

### 6.0.1 Acknowledgements

## References

[1] Zavlin, V. E. 2007, preprint (ArXiv astro-ph/0702426)

[2] Haberl, F. 2007, Ap&SS, 308, 181

[3] Pons, J. A et al. 2002, ApJ, 564, 981

[4] Schwope, A. D. and Hambaryan, V. and Haberl, F. and Motch, C. 2007, Ap&SS, 308, 619

[5] Pérez-Azorín, J. F., Pons, J. A., Miralles, J. A., & Miniutti, G. 2006, A&A, 459, 175

[6] Geppert, U., Küker, M., & Page, D. 2004, A&A, 426, 267

[7] Pérez-Azorín, J. F., Miralles, J. A., & Pons, J. A. 2006, A&A, 451, 1009

[8] Aguilera, D. N., Pons, J. A., & Miralles, J. A., A&A 2008 (in press), 0710.0854 (astro-ph).

[9] Pons, J. A. & Geppert, U. 2007, A&A, 470, 303

[10] Aguilera, D. N., Pons, J. A., & Miralles, J. A. 2008, ApJ Lett., 673, L167

[11] Page, D., Lattimer, J. M., Prakash, M., & Steiner, A. W. 2004, ApJS, 155, 623

[12] Kaspi, V. M. 2007, Ap&SS, 308, 1

[13] Miralles, J. A., Urpin, V., & Konenkov, D. 1998, ApJ, 503, 368